7th ECCOMAS Thematic Conference on Smart Structures and Materials
SMART 2015
A.L. Araúo, C.A. Mota Soares, et al. (Editors)

LATERAL VIBRATION ATTENUATION OF A BEAM WITH CIRCULAR CROSS-SECTION BY SUPPORTS WITH INTEGRATED RESONANTLY SHUNTED PIEZOELECTRIC TRANSDUCERS

Benedict Götz*, **Roland Platz**†, **Tobias Melz***

*Technische Universität Darmstadt, System Reliability and Machine Acoustics SzM
Magdalenenstrasse 4, D-64289, Darmstadt, Germany
goetz@szm.tu-darmstadt.de

†Fraunhofer Institute for Structural Durability and System Reliability LBF
Bartningstrasse 47, D-64289, Darmstadt, Germany

Keywords: vibration attenuation, piezoelectric shunt damping, resonant shunt, beam, circular cross-section

Summary: *Undesired vibration may occur in lightweight structures due to excitation and low damping. For the purpose of vibration attenuation, resonant shunting of piezoelectric transducers can be an appropriate measure. This technique transfers mechanical vibration energy from the mechanical structure into an electrical vibratory system, resulting in reduced vibration of the mechanical structure. In this paper, lateral vibration attenuation in one of the two elastic supports of a beam with circular cross-section by integration of resonantly shunted piezoelectric stack transducers is investigated numerically and experimentally. In the elastic support, bending of the beam is transformed into the stack transducer's axial deformation. For vibration attenuation, resonant shunts including a resistor and an inductance are chosen. It is shown that the concept of an elastic beam support with integrated resonantly shunted piezoelectric stack transducers is capable of reducing the lateral vibration of the beam in arbitrary direction.*

1. INTRODUCTION

Structural vibration may occur in mechanical systems leading to fatigue, reduced durability or undesirable noise. In this context, resonantly shunted piezoelectric transducers can be an appropriate measure. Generally, a piezoelectric transducer converts mechanical kinetic energy of a vibrating host structure into electrical energy. By connecting the electrodes of the transducer to an electrical circuit, the electromechanical impedance of the shunted transducer may achieve vibration attenuation. Shunting the piezoelectric transducer with resistor and inductance, the resonant RL-shunt, an electrical oscillation circuit with the inherent capacitance of the transducer is created. This electromechanical system acts comparable to a mechanical vibration absorber. Vibration attenuation with shunted piezoelectric transducers has been subject to research for several decades [1, 2, 3, 4]. In [3], an overview of shunt damping technologies

such as simple resonant shunts or complex shunts with negative capacitance, [4], and switched shunts, [2], is given. With increasing shunt complexity, enhancements in vibration attenuation and system robustness are pursued.

In mechanical and civil engineering, truss structures that represent complex mechanical systems bear and withstand static and dynamic loads. Truss structures comprise truss members, considered as beams that are connected to each other via the relatively stiff truss supports. Therefore, truss structures show global vibration modes with lateral moving or rotating truss supports. Furthermore, local modes exist that are dominated by the lateral vibration of the truss members. Truss structures that are subject to heavy mass loading may show adequate separation in the structural frequencies of global and local modes. However, dynamics of other truss structure designs may be affected by local modes whose frequencies lie within the bandwidth of the global modes.

For vibration reduction in truss structures, piezoelectric shunt damping has been investigated in [5, 6, 7, 8]. Axial piezoelectric stack transducers are integrated, e. g. in one strut of the truss and investigations are focused on vibrations of global modes, resulting in compression and elongation of the transducer in axial direction of the strut, [5, 6, 8]. Resonant RL-shunts and shunts with negative capacitance were connected to the piezoelectric stack transducers for vibration attenuation. In [6], a smart support with piezoelectric washers has been investigated and vibration attenuation in a truss substructure was achieved.

In this paper, an alternative concept for integrating piezoelectric stack transducers in truss structures for vibration attenuation is presented. The new concept uses an elastic beam support with integrated piezoelectric stack transducers. Bending of the beam in arbitrary direction is transferred to the transducers via a relatively stiff axial extension. Hence, lateral beam vibrations of a truss member as well as global truss structure vibrations can by attenuated. In former studies, e. g. in [8], only global modes could be attenuated. In this paper, only one truss member, an elastically supported beam under harmonic excitation is considered to show that lateral vibration attenuation in arbitrary direction is possible. The concept is investigated numerically and experimentally.

2. SYSTEM DESCRIPTION

The investigated system is an elastically supported beam of length l_b with circular solid cross-section of radius r_b, constant bending stiffness EI_b and density ρ_b, Fig. 1a. The circular cross section has no preferred direction of vibration, so the beam may vibrate in any plane lateral to the x-axis. Elastic spring elements with lateral stiffness $k_{\mathrm{l,A}} = k_{\mathrm{l,B}} = k_\mathrm{l}$ and rotational stiffness $k_{\varphi,\mathrm{A}} = k_{\varphi,\mathrm{B}} = k_\varphi$ in both supports A and B at location $x = 0$ and $x = l_\mathrm{b}$ bear lateral forces at the beam's ends in y- and z-direction and enable rotation around the y- and z-axis, thus, defining centers of rotation. A force $F_\mathrm{d}(t)$ excites the beam at $x_\mathrm{d} = l_\mathrm{b}/2$ with variable angle $0 \leq \alpha_\mathrm{d} \leq \pi/2$ in y-z plane .

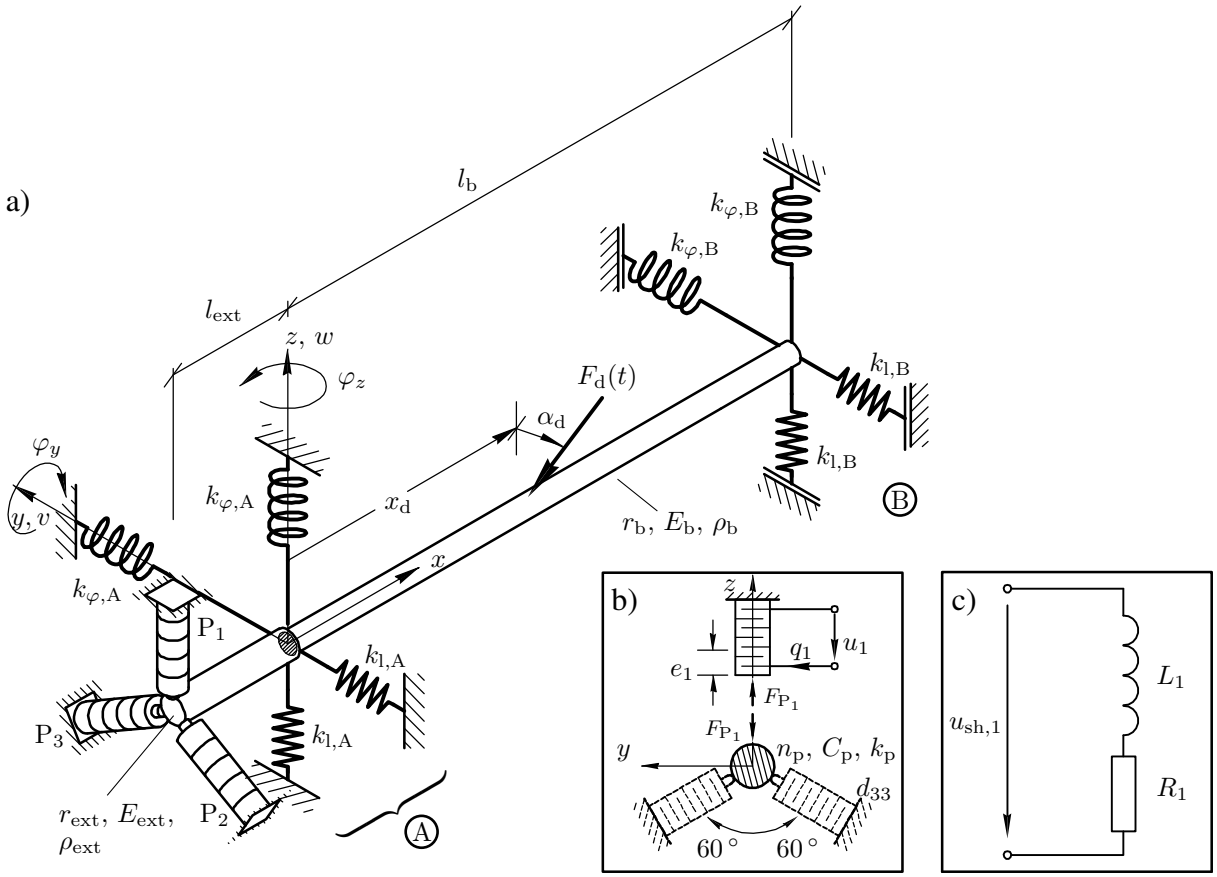

Figure 1: Beam system, a) beam with elastic supports and integrated resonantly shunted piezoelectric stack transducers in support A, b) arrangement of piezoelectric transducers, c) resonant circuit (RL-shunt)

Three transducers in the y-z plane are connected with the center of rotation at the beam's end via a relatively stiff axial extension of length l_ext, radius r_ext, constant bending stiffness EI_ext and density ρ_ext at the support A in Fig. 1a. With that, bending of the beam around the y- and

z-axis is transformed into the stack transducer's axial deformation assuming only small bending deflection at the axial extension's end, so rotational displacements at $x = -l_{\mathrm{ext}}$ are neglected. An elastic spring element and the piezoelectric transducers form the actual beam support A, Fig. 1b. In support A at location $x = -l_{\mathrm{ext}}$, three piezoelectric stack transducers P_1, P_2 and P_3 are arranged in the support housing at an angle of 120° to each other, orthogonal to the beam's longitudinal x-axis in y-z plane. The piezoelectric transducer P_1 affects the axial extension with the lateral force F_{P_1}. The transducer's axial elongation is e_1. The electrical charge at the transducer electrodes is q_1 and the electrical potential difference between the electrodes is the voltage u_1. The properties of each uniaxial transducer are: the number of layers of piezoelectric material n_{p}, the capacitance C_{p} at constant mechanical stress, the piezoelectric constant d_{33} and the mechanical stiffness with short circuited electrodes k_{p}, see Fig. 1b. For vibration reduction in any plane lateral to the x-axis, each piezoelectric transducer is connected to an electrical network with resistance R and inductance L, the RL-shunt, Fig. 1c.

The experimental setup of one elastic support with three piezoelectric stack transducers is shown in Fig. 2a. Fig. 2b shows a sectional view of the CAD model with the piezoelectric stack transducers colored in red, the axial extension colored in blue and the elastic spring element colored in yellow. The support housing and beam material is aluminum alloy EN AW-7075 and the extension is hardened steel 1.2312. The elastic spring element is made of spring steel 1.4310.

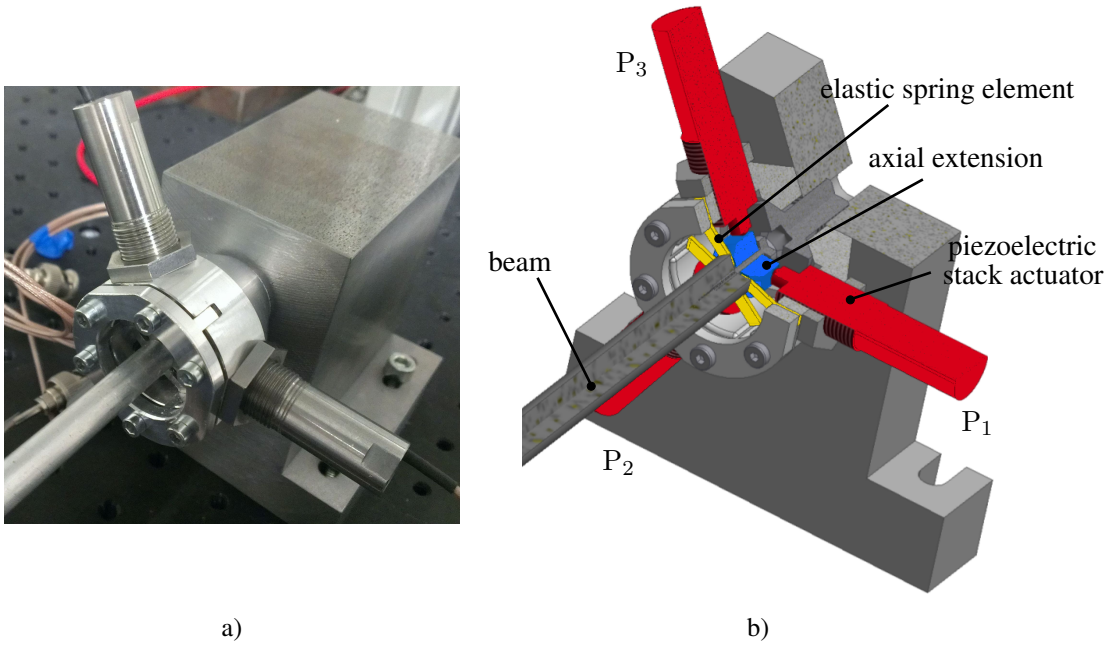

Figure 2: Elastic beam support A with integrated piezoelectric stack transducers P_1, P_2 and P_3 a) experimental setup b) sectional view of CAD model with the stack transducers (red), axial extension (blue) and elastic spring element (yellow)

All properties of the elastically supported beam with piezoelectric stack transducers are given in Table 1.

property	symbol	value	SI-units
beam length	l_b	0.4	m
beam radius	r_b	0.005	m
density aluminum	ρ_b	2775	$\mathrm{kg/m^3}$
Young's modulus aluminum	E_b	$74 \cdot 10^9$	$\mathrm{N/m^2}$
axial extension length	l_ext	0.0075	m
axial extension radius	r_ext	0.006	m
density steel	ρ_ext	7800	$\mathrm{kg/m^3}$
Young's modulus steel	E_ext	$210 \cdot 10^9$	$\mathrm{N/m^2}$
stiffness of piezoelectric transducer	k_p	$22 \cdot 10^6$	$\mathrm{N/m}$
lateral stiffness of spring element	k_l	$49.74 \cdot 10^6$	$\mathrm{N/m}$
rotational stiffness of spring element	k_φ	273	$\mathrm{Nm/rad}$
piezoelectric coefficient	d_{33}	$640 \cdot 10^{-12}$	$\mathrm{m/V}$
number of layers in stack transducer	n_p	340	–
capacitance of stack transducer	C_p	$3.55 \cdot 10^{-6}$	F

Table 1: Geometric, material and electromechanical properties

3. MATHEMATICAL MODEL

In this section, the derivation of a mathematical model for simulating the lateral vibration in y- and z-direction of the elastically supported beam with resonantly shunted stack transducers, as described in Sec. 2., is presented. In a first step, a finite element (FE) model of the beam is developed. In a second step, three resonantly shunted piezoelectric stack transducers are connected to the beam. Finally, a linear state space formulation of the coupled electromechanical system is derived in the LAPLACE domain and transformed into frequency domain to calculate the frequency transfer function of the harmonically excited beam with resonantly shunted transducers.

3.1 Finite element model

To describe the lateral vibration of the beam in y- and z-direction, a FE model of the system presented in Sec. 2. is used.

The beam and the axial extension are discretized by $N-1=11$ one-dimensional EULER-BERNOULLI beam elements, see Fig. 3a, with $N=12$ nodes and four degrees of freedom per node, see Fig. 3b. Each node n has two translational displacements v_n and w_n in y- and z-direction and two rotational displacements φ_{y_n} and φ_{z_n} around the y- and z-axis. In order to build the element stiffness and element mass matrices, the GALERKIN method is used, [9].

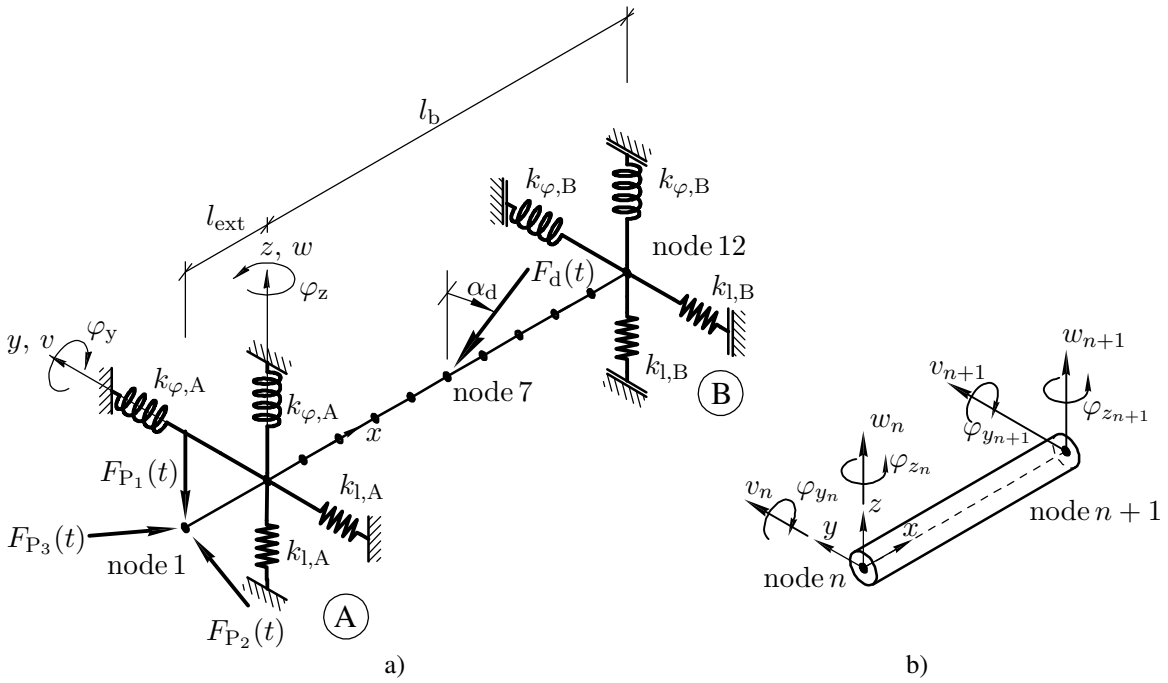

Figure 3: a) FE model of elastically supported beam with 12 nodes, forces $F_{\mathrm{P}_1}(t)$, $F_{\mathrm{P}_2}(t)$ and $F_{\mathrm{P}_3}(t)$ of the piezoelectric transducers P_1, P_2 and P_3 and excitation force $F_\mathrm{d}(t)$, b) finite beam element between node n and $n+1$ with element coordinates in positive directions

For bending, HERMITIAN cubic shape functions are used for y- and z-direction. The resulting $[8 \times 8]$ elastic element stiffness matrix $\mathbf{K}_\mathrm{el}$ and element mass matrix $\mathbf{M}_\mathrm{el}$ are found in literature, [9, 10].

After assembling global stiffness and mass matrices from the element matrices, the global equation of motion system of the elastically supported beam in Fig. 3a is

$$\mathbf{M}\,\ddot{\mathbf{x}}(t) + \mathbf{D}\,\dot{\mathbf{x}}(t) + \mathbf{K}\,\mathbf{x}(t) = \mathbf{F}_\mathrm{d}(t) - \mathbf{F}_\mathrm{p}(t). \tag{1}$$

The $[4N \times 1]$ global displacement vector is given by

$$\mathbf{x}(t) = \left[v_1(t), w_1(t), \varphi_{y1}(t), \varphi_{z1}(t), ..., v_N(t), w_N(t), \varphi_{y_N}(t), \varphi_{z_N}(t)\right]^T. \tag{2}$$

$\mathbf{M}$, $\mathbf{D}$ and $\mathbf{K}$ are the global mass matrix, damping matrix and stiffness matrix with dimension $[4N \times 4N]$. The external force vector is

$$\mathbf{F}_\mathrm{d}(t) = \mathbf{b}_\mathrm{d}\,F_\mathrm{d}(t) = [\mathbf{0}^{[1\times 4(N-6)]}, -\cos(\alpha_\mathrm{d}), \cos(\alpha_\mathrm{d}), 0, 0, \mathbf{0}^{[1\times 4(N-7)]}]^T\,F_\mathrm{d}(t) \tag{3}$$

with $\mathbf{b}_\mathrm{d}$ mapping the excitation force $F_\mathrm{d}(t)$ to node 7. $\mathbf{F}_\mathrm{p}(t)$ is the resulting $[4N \times 3]$ piezoelectric transducer force vector from the three transducers P_1, P_2 and P_3, see Sec. 3.2. Proportional

damping is given by $\mathbf{D} = \alpha\,\mathbf{M} + \beta\,\mathbf{K}$, [11]. The proportional damping coefficients α and β are determined for modal damping ratios of the first and second mode $\zeta_{1/2} = 0.5\%$ obtained from experiment. The lateral stiffness $k_{\mathrm{l,A/B}}$ in y-and z-direction and the rational stiffness $k_{\varphi,\mathrm{A/B}}$ around y- and z-axis of the elastic spring elements at location $x = 0$ and $x = l_{\mathrm{b}}$ are added to the global stiffness matrix at nodes $n = 2$ and $n = 12$.

3.2 Mathematical model of elastically supported beam with stack transducers

To describe the effect of piezoelectric transducers on the lateral beam vibration, a linear mathematical transducer model is derived. In the following, all transducer properties number of layers n_{p}, piezoelectric coefficient d_{33}, stiffness k_{p} and capacitance C_{p} according to Table 1 are the same for each transducer P_1, P_2 and P_3. The transducer forces in support A $\mathbf{F}_{\mathrm{p,A}}(t) = [F_{\mathrm{P}_1}(t), F_{\mathrm{P}_2}(t), F_{\mathrm{P}_3}(t)]^T$ are calculated with the transducers axial elongations $\mathbf{e}(t) = [e_1(t), e_2(t), e_3(t)]^T$ and the voltages $\mathbf{u}(t) = [u_1(t), u_2(t), u_3(t)]^T$ that are applied across the transducer electrodes,

$$\mathbf{F}_{\mathrm{p,A}}(t) = k_{\mathrm{p}}\,\mathbf{e}(t) - \Theta\,\mathbf{u}(t). \tag{4}$$

In (4), $\Theta = n_{\mathrm{p}}\,d_{33}\,k_{\mathrm{p}}$. The charges $\mathbf{q}(t) = [q_1(t), q_2(t), q_3(t)]^T$ at the transducer electrodes are calculated with the transducers axial elongations $\mathbf{e}(t)$ and the voltages $\mathbf{u}(t)$ applied across the transducer electrodes,

$$\mathbf{q}(t) = \Theta\,\mathbf{e}(t) + C_{\mathrm{p}}\,\mathbf{u}(t). \tag{5}$$

The forces $\mathbf{F}_{\mathrm{p,A}}(t)$ of all piezoelectric transducers acting on the axial extension at support A, see Fig. 3a, are considered in the piezoelectric transducer force vector

$$\mathbf{F}_{\mathrm{p}}(t) = \mathbf{B}_{\mathrm{p}}\,\mathbf{F}_{\mathrm{p,A}}(t). \tag{6}$$

The $[4N \times 3]$ matrix $\mathbf{B}_{\mathrm{p}}$ maps the transducer forces according their effective direction to node 1. $\mathbf{B}_{\mathrm{p}} = [\mathbf{b}_1; \mathbf{b}_2; \mathbf{b}_3]$ with

$$\begin{aligned}\mathbf{b}_1 &= \left[0, -1, 0, 0, \mathbf{0}^{1\times 4(N-1)}\right]^T,\ \mathbf{b}_2 = \left[\sin(60°), \cos(60°), 0, 0, \mathbf{0}^{1\times 4(N-1)}\right]^T \text{ and} \\ \mathbf{b}_3 &= \left[-\sin(60°), \cos(60°), 0, 0, \mathbf{0}^{1\times 4(N-1)}\right]^T.\end{aligned} \tag{7}$$

Angles of $60°$ are formed in Fig. 1b due to the transducer arrangement. Similarly, the axial transducer elongations $\mathbf{e}(t)$ are related to the displacements $v_1(t)$ and $w_1(t)$ in y- and z-direction at node 1 by

$$\mathbf{e}(t) = \mathbf{B}_{\mathrm{p}}^T\,\mathbf{x}(t). \tag{8}$$

Replacing $\mathbf{e}(t)$ in (4) by (8) and substituting $\mathbf{F}_{\mathrm{p,A}}(t)$ in (6) by (4), the piezoelectric force vector

$$\mathbf{F}_{\mathrm{p}}(t) = k_{\mathrm{p}}\,\mathbf{B}_{\mathrm{p}}\,\mathbf{B}_{\mathrm{p}}^T\,\mathbf{x}(t) - \Theta\,\mathbf{B}_{\mathrm{p}}\,\mathbf{u}(t). \tag{9}$$

Inserting (9) in (1), the beam equation of motion system with voltage driven transducers is

$$\mathbf{M}\,\ddot{\mathbf{x}}(t) + \mathbf{D}\,\dot{\mathbf{x}}(t) + \mathbf{K}\,\mathbf{x}(t) + k_{\mathrm{p}}\,\mathbf{B}_{\mathrm{p}}\,\mathbf{B}_{\mathrm{p}}^T\mathbf{x}(t) - \Theta\,\mathbf{B}_{\mathrm{p}}\,\mathbf{u}(t) = \mathbf{F}_{\mathrm{d}}(t). \tag{10}$$

Furthermore, replacing $\mathbf{e}(t)$ in (5) with (8), the charges at the transducer electrodes are calculated from

$$\mathbf{q}(t) = \Theta\, \mathbf{B}_\mathrm{p}^T\, \mathbf{x}(t) + C_\mathrm{p}\, \mathbf{u}(t). \tag{11}$$

The coupled matrix equation of motion system of beam with piezoelectric transducers, see Fig. 3a, are represented by (10) and (11).

3.2.1 Effect of piezoelectric transducers on beam eigenfrequencies

For vibration attenuation via shunted transducers, the system's angular eigenfrequencies are an important measure. To investigate the influence of piezoelectric transducers on the beam system stiffness and, thus, on the beam system angular eigenfrequencies, three eigenvalue problems can be distinguished by analyzing (1), (10) and (11) for neglected excitation force $\mathbf{F}_\mathrm{d}(t) = 0$ and small damping that is neglected, $\mathbf{D} = 0$:

- if no transducer is connected to the beam $\mathbf{F}_\mathrm{p}(t) = 0$, the angular eigenfrequencies ω_b of the beam are calculated by solving

$$\det\left[\mathbf{K} - \omega_\mathrm{b}^2\, \mathbf{M}\right] = 0 \tag{12}$$

- if transducers are connected to the beam $\mathbf{F}_\mathrm{p}(t) \neq 0$ and $\mathbf{u}(t) = 0$, i. e. the electrodes of the transducer are short circuited (sc) and the transducer stiffness with short circuited electrodes is taken into account, (10) becomes

$$\mathbf{M}\, \ddot{\mathbf{x}}(t) + \mathbf{K}\, \mathbf{x}(t) + k_\mathrm{p}\, \mathbf{B}_\mathrm{p}\, \mathbf{B}_\mathrm{p}^T \mathbf{x}(t) = \mathbf{M}\, \ddot{\mathbf{x}}(t) + \mathbf{K}_\mathrm{sc}\, \mathbf{x}(t) = 0, \tag{13}$$

$$\mathbf{K}_\mathrm{sc} = \mathbf{K} + k_\mathrm{p}\, \mathbf{B}_\mathrm{p}\, \mathbf{B}_\mathrm{p}^T \tag{14}$$

  and the angular eigenfrequencies ω_sc are calculated by solving

$$\det\left[\mathbf{K}_\mathrm{sc} - \omega_\mathrm{sc}^2\, \mathbf{M}\right] = 0 \tag{15}$$

- if transducers are connected to the beam $\mathbf{F}_\mathrm{p}(t) \neq 0$ and $\mathbf{q}(t) = 0$, i. e. the electrodes of the transducer are open circuited (oc) and the transducer stiffness with open circuited electrodes is taken into account, (10) and (11) result in

$$\mathbf{M}\, \ddot{\mathbf{x}}(t) + \mathbf{K}\, \mathbf{x}(t) + \left(k_\mathrm{p} + \frac{\Theta^2}{C_\mathrm{p}}\right) \mathbf{B}_\mathrm{p}\, \mathbf{B}_\mathrm{p}^T \mathbf{x}(t) = \mathbf{M}\, \ddot{\mathbf{x}}(t) + \mathbf{K}_\mathrm{oc}\, \mathbf{x}(t) = 0, \tag{16}$$

$$\mathbf{K}_\mathrm{oc} = \mathbf{K}_\mathrm{sc} + \frac{\Theta^2}{C_\mathrm{p}}\, \mathbf{B}_\mathrm{p}\, \mathbf{B}_\mathrm{p}^T. \tag{17}$$

  and the angular eigenfrequencies ω_oc are calculated by solving

$$\det\left[\mathbf{K}_\mathrm{oc} - \omega_\mathrm{oc}^2\, \mathbf{M}\right] = 0. \tag{18}$$

3.2.2 General electromechanical coupling coefficient

For vibration reduction with shunt damping, the generalized electromechanical coupling coefficient K_{33} is an important measure to evaluate the vibration attenuation capability. It characterizes the energy exchanged between the mechanical and the electrical domains of the piezoelectric transducer coupled to the structure. The coupling coefficient K_{33} may be calculated with the short and open circuited angular eigenfrequencies ω_{sc} and ω_{oc}, [12], to

$$K_{33} = \sqrt{\frac{\omega_{\mathrm{oc}}^2 - \omega_{\mathrm{sc}}^2}{\omega_{\mathrm{oc}}^2}}. \tag{19}$$

3.3 Mathematical model of elastically supported beam with resonantly shunted stack transducers

To describe the effect of resonantly shunted piezoelectric transducers on the lateral beam vibration, linear resistive inductive shunts are taken into account. A shunt with resistance R and inductance L is connected to the piezoelectric stack transducer P_1, P_2 and P_3, Fig. 1c. Using the second KIRCHOFF's law, the voltages across the shunt terminals for all three transducers P_1, P_2 and P_3

$$\mathbf{u}_{\mathrm{sh}}(t) = \begin{bmatrix} -L_1 & & \\ & -L_2 & \\ & & -L_3 \end{bmatrix} \ddot{\mathbf{q}}(t) + \begin{bmatrix} -R_1 & & \\ & -R_2 & \\ & & -R_3 \end{bmatrix} \dot{\mathbf{q}}(t) \tag{20}$$

Solving (11) for $\mathbf{u}(t)$ and substituting $\mathbf{u}(t)$ in (10), the shunt is connected to the transducer electrodes. Furthermore, replacing $\mathbf{u}(t)$ in (11) by (20) with $\mathbf{u}(t) = \mathbf{u}_{\mathrm{sh}}(t)$, the coupled equation of motion system of the beam with resonantly shunted stack transducers (sh) is

$$\mathbf{M}_{\mathrm{sh}}\, \ddot{\mathbf{x}}_{\mathrm{sh}}(t) + \mathbf{D}_{\mathrm{sh}}\, \dot{\mathbf{x}}_{\mathrm{sh}}(t) + \mathbf{K}_{\mathrm{sh}}\, \mathbf{x}_{\mathrm{sh}}(t) = \mathbf{b}_{\mathrm{sh}}\, F_{\mathrm{d}}(t) \tag{21}$$

with the parameter matrices

$$\mathbf{M}_{\mathrm{sh}} = \left[\begin{array}{c|ccc} \mathbf{M} & & & \\ \hline & L_1 & & \\ & & L_2 & \\ & & & L_3 \end{array}\right], \quad \mathbf{D}_{\mathrm{sh}} = \left[\begin{array}{c|ccc} \mathbf{D} & & & \\ \hline & R_1 & & \\ & & R_2 & \\ & & & R_3 \end{array}\right], \tag{22}$$

$$\mathbf{K}_{\mathrm{sh}} = \left[\begin{array}{c|ccc} \mathbf{K}_{\mathrm{oc}} & & -\frac{\Theta}{C_{\mathrm{p}}}\mathbf{B}_{\mathrm{p}} & \\ \hline & 1/C_{\mathrm{p}} & & \\ -\frac{\Theta}{C_{\mathrm{p}}}\mathbf{B}_{\mathrm{p}}^T & & 1/C_{\mathrm{p}} & \\ & & & 1/C_{\mathrm{p}} \end{array}\right] \quad \text{and} \quad \mathbf{b}_{\mathrm{sh}} = \begin{bmatrix} \mathbf{b}_{\mathrm{d}} \\ 0 \\ 0 \\ 0 \end{bmatrix}. \tag{23}$$

and the time domain solution $\mathbf{x}_{\mathrm{sh}}(t) = \left[\mathbf{x}(t)^T, \mathbf{q}(t)^T\right]^T$.

3.4 Frequency transfer behavior of elastically supported beam with resonantly shunted stack transducers

To describe the lateral beam vibration with resonantly shunted transducers in y- and z-direction in frequency domain, a first order state space model is derived from (21). For later investigations, only the transfer behavior of force F_d at node 7 to lateral displacements v_7 and w_7 at node 7 are considered. Therefore, the state space model of the electromechanical system in LAPLACE domain with LAPLACE variable s can be written, [13] , as

$$\begin{aligned} s\,\mathbf{z}(s) &= \mathbf{A}\,\mathbf{z}(s) + \mathbf{B}\,F_\mathrm{d}(s) \\ \mathbf{y}(s) &= \mathbf{C}\,\mathbf{z}(s) + D\,F_\mathrm{d}(s) \end{aligned} \tag{24}$$

with system matrix $\mathbf{A}$, input matrix $\mathbf{B}$, output matrix $\mathbf{C}$ and feedthrough constant $D = 0$,

$$\mathbf{A} = \begin{bmatrix} \mathbf{0}^{[(4N+3)\times(4N+3)]} & \mathbf{I}^{[(4N+3)\times(4N+3)]} \\ -\mathbf{M}_\mathrm{sh}^{-1}\,\mathbf{D}_\mathrm{sh} & -\mathbf{M}_\mathrm{sh}^{-1}\,\mathbf{K}_\mathrm{sh} \end{bmatrix}, \quad \mathbf{B} = \begin{bmatrix} \mathbf{0}^{[(4N+3)\,\times\,1]} \\ \mathbf{M}_\mathrm{sh}^{-1}\,\mathbf{b}_\mathrm{sh} \end{bmatrix} \quad \text{and} \tag{25}$$

$$\mathbf{C} = \left[\begin{array}{c:c} \begin{matrix} [\mathbf{0}^{[1\times 4(N-6)]}, 1, 0, 0, 0, \mathbf{0}^{[1\times(4(N-7)+3)]}] \\ \mathbf{0}^{[1\times 4(N-6)]}, 0, 1, 0, 0, \mathbf{0}^{[1\times(4(N-7)+3)]}] \end{matrix} & \mathbf{0}^{[2\times(4N+3)]} \end{array}\right]. \tag{26}$$

All state variables are contained in the state vector $\mathbf{z}(s)$ and the output vector is $\mathbf{y}(s)$,

$$\mathbf{z}(s) = \begin{bmatrix} \mathbf{x}(s) \\ \mathbf{q}(s) \\ s\,\mathbf{x}(s) \\ s\,\mathbf{q}(s) \end{bmatrix} \quad \text{and} \quad \mathbf{y}(s) = \begin{bmatrix} v_7(s) \\ w_7(s) \end{bmatrix}. \tag{27}$$

The transfer functions of the beam with stack transducers and resonant shunts in LAPLACE domain, [13], result in

$$\mathbf{H}(s) = \frac{\mathbf{y}(s)}{F_\mathrm{d}(s)} = \mathbf{C}(s\,\mathbf{I} - \mathbf{A})^{-1}\mathbf{B} + D. \tag{28}$$

For later comparison with experimental results, the transfer function due to excitation force $F_\mathrm{d}(t)$ and acceleration response in y-direction at node 7 with $\alpha_\mathrm{d} = \pi$ according to Fig. 1

$$H_\mathrm{y}(s) = s^2\frac{v_7(s)}{F_\mathrm{d}(s)} \tag{29}$$

and the transfer function due to excitation force $F_\mathrm{d}(t)$ and acceleration response in z-direction at node 7 with $\alpha_\mathrm{d} = 0$ according to Fig. 1

$$H_\mathrm{z}(s) = s^2\frac{w_7(s)}{F_\mathrm{d}(s)}. \tag{30}$$

In all following figures, H_y and H_z are plotted as functions of frequency f in Hz using the conversion $s = j\,2\pi f$.

4. NUMERICAL INVESTIGATION OF THE INFLUENCE OF SUPPORT PROPERTIES ON THE SHUNT DAMPING CAPABILITY

An numerical investigation is conducted to prove the capability of reducing lateral beam vibrations in y- and z-direction by an elastic support with integrated resonantly shunted piezoelectric stack transducers, introduced in Fig. 1. The rotational support stiffness $k_{\varphi,\mathrm{A}}$ and lateral stiffness $k_{\mathrm{l,A}}$ as well as the axial extension length l_{ext} influence the resulting support stiffness of support A and, thus, the vibration attenuation capability of shunted transducers integrated in support A. Three cases I, II and III, see Table 2, are distinguished to investigate shunt damping capability. Case I investigates the influence of varying $k_{\varphi,\mathrm{A}}$ on the beam's eigenfrequency f_{b} without piezoelectric transducers, on the beam's eigenfrequency f_{sc} with piezoelectric transducers and short circuited electrodes and on the beam's eigenfrequency f_{oc} with transducers and open circuited electrodes. Case II investigates the influence of varying $k_{\mathrm{l,A}}$ on the electromechanical coupling coefficient K_{33} and case III investigates the influence of varying l_{ext} on the electromechanical coupling coefficient K_{33}.

case	I	II	III
varied input	$k_{\varphi,\mathrm{A}}$	$k_{\mathrm{l,A}}$	l_{ext}
investigated output	f_{b}, f_{sc}, f_{oc}	K_{33}	K_{33}

Table 2: Investigated input and output parameters for numerical investigation of vibration reduction capability of support A for cases I, II and III

The vibration behavior of the elastically supported beam with transducers integrated in support A is assumed to be linear and symmetric in y- and z-direction. Hence, numerical investigations in case I, II and III are only conducted for the z-direction.

4.1 Numerical results of cases I, II and III

Case I: To investigate only the influence of varying $k_{\varphi,\mathrm{A}}$ on the eigenfrequency f_{b}, f_{sc} and f_{oc}, the lateral stiffness $k_{\mathrm{l,A}}$ is assumed to be infinite and the rotational stiffness $k_{\varphi,\mathrm{B}}$ in support B is constant with $k_{\varphi,\mathrm{B}} = k_{\varphi}$. In the following, the normalized resulting rotational support stiffness around the y-axis of support A with three integrated piezoelectric transducers is assumed to be

$$k_{\varphi,\mathrm{res}} = \frac{k_{\varphi,\mathrm{A}} + k_z\, l_{\mathrm{ext}}^2}{EI_{\mathrm{b}}/l_{\mathrm{b}}} \quad \text{for} \quad 10^{-3} \leq k_{\varphi,\mathrm{res}} \leq 10^{4}. \tag{31}$$

In (31), k_z is the resulting stiffness of piezoelectric transducers in z-direction. $k_z = 0$ for the elastically supported beam with no transducers, $k_z = 1.5\, k_{\mathrm{p}}$ with short circuited transducer electrodes, (13), or $k_z = 1.5\,(k_{\mathrm{p}} + \Theta^2/C_{\mathrm{p}})$ with open circuited transducer electrodes, (16). Fig. 4 shows the eigenfrequency f_{sc}, (15), and eigenfrequency f_{oc}, (18), for rotational stiffness $k_{\varphi,\mathrm{A}} = [0\, k_{\varphi}; 1\, k_{\varphi}; 6\, k_{\varphi}; 40\, k_{\varphi}]$. With increasing $k_{\varphi,\mathrm{A}}$, the eigenfrequencies for short and open

circuit f_{sc} and f_{oc} move closer together, thus, reducing the coupling coefficient K_{33}, (19). In case $k_{\varphi,\mathrm{A}} = 0\,k_{\varphi}$, $K_{33} = 0.17$ and in case $k_{\varphi,\mathrm{A}} = 40\,k_{\varphi}$, $K_{33} = 0.03$. Meaning that with almost infinite rotational support stiffness $k_{\varphi,\mathrm{A}}$, the coupling coefficient tends to zero. To evaluate the resulting rotational support stiffness $k_{\varphi,\mathrm{res}}$ of support A in comparison to an ideal rotational support at the beam's end, Fig. 4 shows the beam's first eigenfrequency f_{b}, (12), for rotational support stiffness conditions that vary from pinned-elastic with $k_{\varphi,\mathrm{A,res}} = 10^{-3}$ to fixed-elastic with $k_{\varphi,\mathrm{A,res}} = 10^{4}$. The first eigenfrequency of the pinned-elastic beam is $f_{\mathrm{b}} = 156.6\,\mathrm{Hz}$ and for the fixed-elastic beam it is $f_{\mathrm{b}} = 225.8\,\mathrm{Hz}$. For $k_{\varphi,\mathrm{A}} = 0\,k_{\varphi}$, support A represents an elastic support and for $k_{\varphi,\mathrm{A}} = 40\,k_{\varphi}$, support A represents a fixed support.

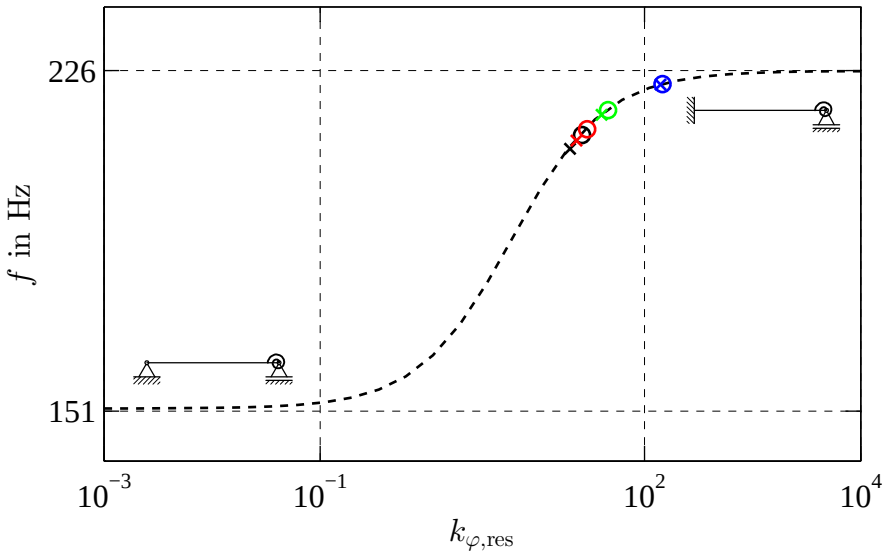

Figure 4: First eigenfrequency f_{b} in z-direction of elastically supported beam without transducers for support conditions pinned-elastic to fixed-elastic (– –), eigenfrequencies of beam with short circuited transducer electrodes f_{sc} (×) and with open circuited transducer electrodes f_{oc} (○) for rational support stiffness $k_{\varphi,\mathrm{A}} = 0\,k_{\varphi}$ (× , ○), $k_{\varphi,\mathrm{A}} = 1\,k_{\varphi}$ (× , ○), $k_{\varphi,\mathrm{A}} = 6\,k_{\varphi}$ (× , ○) and $k_{\varphi,\mathrm{A}} = 40\,k_{\varphi}$ (× , ○)

Case II: In Fig. 5a, the influence of varying lateral support stiffness $k_{\mathrm{l,A}}$ on the coupling coefficient K_{33} is presented for constant rational support stiffness $k_{\varphi,\mathrm{A}} = [0\,k_{\varphi}; 1\,k_{\varphi}; 6\,k_{\varphi}; 40\,k_{\varphi}]$. It is seen that the coupling coefficient is maximal for $k_{\varphi,\mathrm{A}} = 0\,k_{\varphi}$ and $k_{\mathrm{l,A}} = 10 \cdot 10^{10}\,\mathrm{N/m}$ and the coupling coefficient is zero for $k_{\varphi,\mathrm{A}} = 40\,k_{\varphi}$ and $k_{\mathrm{l,A}} = 15.7 \cdot 10^{6}\,\mathrm{N/m}$. With high lateral stiffness $k_{\mathrm{l,A}}$, the center of rotation in support A lies at $x = 0$ in the middle of the spring element. With decreasing stiffness $k_{\mathrm{l,A}}$, the center of rotation in support A is moving from $x = 0$ closer to the transducers, hence, reducing the coupling coefficient K_{33}. The lateral stiffness $k_{\mathrm{l,A}} = 49.74 \cdot 10^{6}\,\mathrm{N/m}$ appears to be an appropriate value for a significant shunt damping capability and is shown in Fig. 5a.

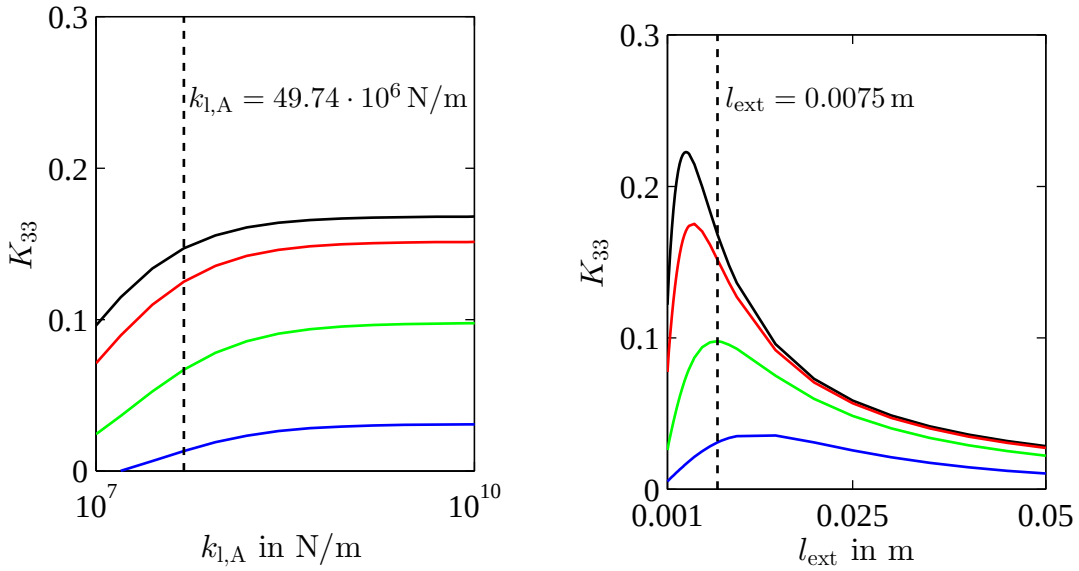

Figure 5: Electromechanical coupling coefficient K_{33} influenced by a) varying lateral stiffness $k_{\mathrm{l,A}}$ and b) varying extension length l_{ext}, values of constant rotational stiffness $k_{\varphi,\mathrm{A}} = 0\,k_\varphi$ (—), $k_{\varphi,\mathrm{A}} = 1\,k_\varphi$ (—), $k_{\varphi,\mathrm{A}} = 6\,k_\varphi$ (—) and $k_{\varphi,\mathrm{A}} = 40\,k_\varphi$ (—)

Case III: In Fig. 5b, the influence of varying axial extension length l_{ext} on the coupling coefficient K_{33} is presented for different constant rotational stiffness $k_{\varphi,\mathrm{A}} = [0\,k_\varphi; 1\,k_\varphi; 6\,k_\varphi; 40\,k_\varphi]$. The coupling coefficient K_{33} can be maximized by adjusting the value for l_{ext}. For $k_{\varphi,\mathrm{A}} = 0\,k_\varphi$ and $l_{\mathrm{ext}} = 0.0035\,\mathrm{m}$, the coupling coefficient is maximal and $K_{33} = 0.22$. Furthermore, the reachable maximum of K_{33} is, again, reduced with increasing $k_{\varphi,\mathrm{A}}$ and shifts to higher values of l_{ext}. The extension length $l_{\mathrm{ext}} = 0.0075\,\mathrm{m}$ was chosen due to design constraints. According to Fig. 5b, this extension length appears to be sufficient for an effective shunt damping capability.

In Fig. 5a and Fig. 5b, the coupling coefficient $K_{33} = 0.13$ for $k_{\varphi,A} = 273\,\mathrm{Nm/rad}$ with $k_{\mathrm{l,A}} = 49.74 \cdot 10^6\,\mathrm{N/m}$ and $l_{\mathrm{ext}} = 0.0075\,\mathrm{m}$, see Table 1. These combinations lead to an adequate electromechanical coupling and are chosen in the following for numerical and experimental vibration attenuation investigations.

5. VIBRATION REDUCTION OF BEAM WITH ELASTIC SUPPORTS AND INTEGRATED RESONANTLY SHUNTED TRANSDUCERS

In this section, the vibration reduction of a beam with elastic supports A and B and integrated resonantly shunted piezoelectric transducers in support A is investigated numerically and experimentally for properties given in Table 1. Therefore, the frequency transfer functions $|H_y|$ and $|H_z|$ in y- and z-direction, according to (29) and (30), with open circuited transducer

electrodes and RL-shunt are presented. In the experiment, an electrodynamic shaker is used for excitation and the excitation force $F_{\mathrm{d}}(t)$ and the accelerations $\ddot{v}_7(t)$ and $\ddot{w}_7(t)$ at x_{d} are measured via an impedance head.

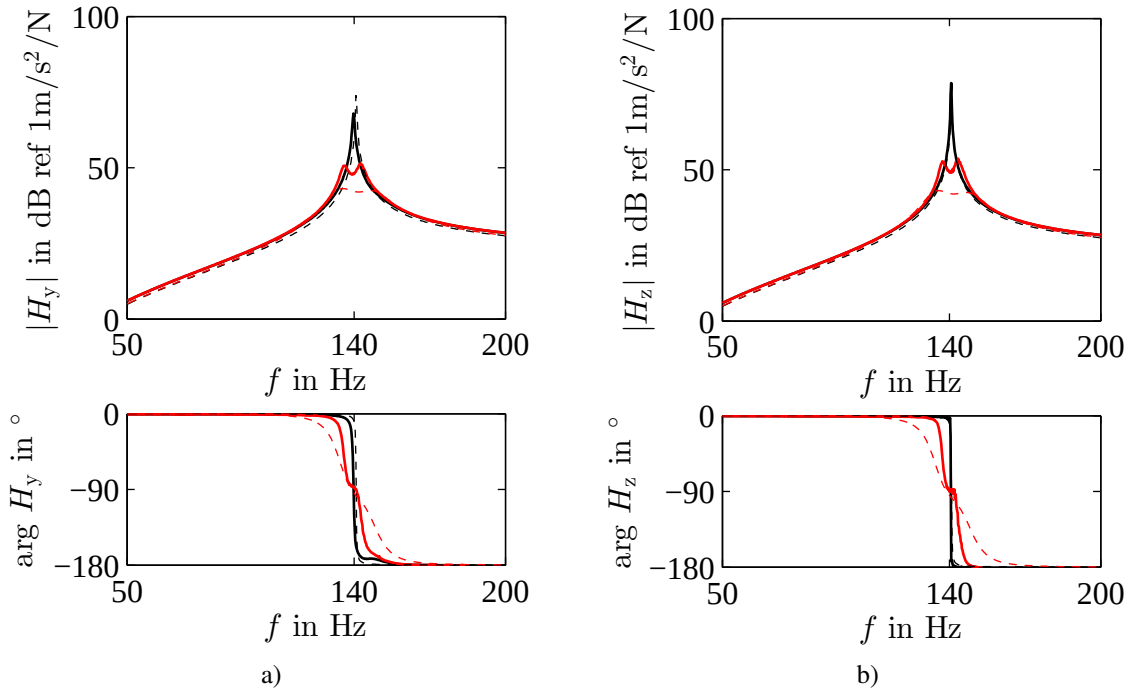

Figure 6: Frequency transfer behavior of the beam with elastic supports and three integrated resonantly shunted piezoelectric transducers in support A with open circuited electrodes: simulation (– –) and experiment (——) and with RL-shunt: simulation (– –) and experiment (——) in a) y-direction and b) z-direction

Fig. 6a and Fig. 6b show the vibration behavior at node 7 of the beam in y- and z-direction for the numerical simulation with open circuited transducer electrodes and with connected RL-shunt. For the experimental setup it is also shown with open circuited transducer electrodes and with connected RL-shunt. For the numerical simulation, the vibration reduction in y-direction and z-direction is $31\,\mathrm{dB}$ since symmetry is assumed. For the experimental setup, the vibration reduction in y-direction is only $16\,\mathrm{dB}$ and in z-direction is only $26\,\mathrm{dB}$. What is more, non symmetric experimental behavior is observed. The difference between numerical and experimental vibration reduction is presumably due to a smaller coupling coefficient in the experiment. In the numerical simulation, $K_{33} = 0.13$ and in the experiment, $K_{33} = 0.03$. That, in turn, may result from an overestimate lateral stiffness $k_{\mathrm{l,A}}$ in the simulation, which has a significant influence on the coupling coefficient, see Sec. 4.1. The reduced vibration reduction in the experiment compared to the numerical results may also be observed in the phase $\arg H_{y/z}$. Furthermore in the experiment, the eigenfrequency $f_{\mathrm{oc}} = 139.8\,\mathrm{Hz}$ in y-direction and $f_{\mathrm{oc}} = 140.8\,\mathrm{Hz}$ in

z-direction. This is due to non symmetric rotational support stiffness k_φ and bending stiffness EI_b. Still the effect is relatively small and assuming symmetric vibration behavior in y- and z-direction in the numerical simulation is justified.

6. CONCLUSIONS

Lateral vibration reduction of a beam with circular cross-section in one of the beam's two elastic supports by integration of resonantly shunted piezoelectric transducers is investigated numerically and experimentally. The vibration attenuation via RL-shunts depends significantly on the electromechanical coupling coefficient. The electromechanical coupling coefficient is, again, significantly dependent on the rotational stiffness and the lateral support stiffness of the elastic spring element. The coupling coefficient is maximal if there is a very small rotational stiffness and zero for infinite high rotational stiffness. Reducing the lateral stiffness, also decreases the coupling coefficient. Furthermore, the coupling coefficient can be maximized by adjusting the axial extension length at constant rotational stiffness. An experimental setup of the elastically supported beam with integrated piezoelectric stack transducers in the elastic support is presented and a significantly lateral vibration reduction is achieved with resonant shunt damping in both lateral directions y and z. However, the experiments show less vibration reduction capability than the numerical simulation. What is more, non symmetric behavior is observed in the supports in horizontal and vertical direction experimentally. The relatively small electromechanical coupling coefficient in the experimental setup could be improved by a different design of the elastic spring element with higher lateral stiffness. Additional investigations will be conducted to examine the influence of the support housing stiffness. Furthermore, the vibration reduction could be improved by adding a negative capacitance to the RL-shunt.

7. ACKNOWLEDGMENTS

The authors like to thank the German Research Foundation (DFG) for funding this research within the Collaborative Research Center (SFB) 805.

References

[1] Hagood, N. W. and von Flotow, A., Damping of structural vibrations with piezoelctric materials and passive electrical networks. *Journal of Sound and Vibration*, 146(2): 243–268, 1991.

[2] Niederberger, D. *Smart Damping Materials using Shunt Control*. Ph.D. thesis, Swiss Federal Institute of Technology Zürich, 2005.

[3] Moheimani, S. O. R. and Fleming, A. J., *Piezoelectric Transducers for Vibration Control and Damping*. Springer-Verlag London, 2006.

[4] Beck, B. S., *Negative Capacitance Shunting of Piezoelectric Patches for Vibration Control of Continuous Systems*. Ph.D. thesis, Georgia Institute of Technology, 2012.

[5] Hagood, N. W. and Crawley, E. F., Experimental investigation of passive enhancement of damping for space structures. *Journal of Guidance, Control, and Dynamics*, 14(6): 1100 – 1109, November 1991.

[6] Hagood, N. W., Aldrich, J. B. and von Flotow, A. H., Design of passive piezoelectric damping for space structures. *NASA Contractor Report*, 4625, 1994.

[7] Lammering, R., Jia, J. and Rogers, C. A., Optimal placement of piezoelectric actuators in adaptive truss structures. *Journal of Sound and Vibration*, 171(1): 67–85, 1994.

[8] Preumont, A., de Marneffe, B., Deraemaeker, A., and Bossens, F., The damping of a truss structure with a piezoelectric transducer. *Computers & Structures*, 86: 227 – 239, 2008.

[9] Klein, B., *FEM*. Number 978-3-8348-2134-8. Vieweg & Teubner, GWV Fachverlage GmbH Springer Fachmedien Wiesbaden GmbH, 2012.

[10] Przemieniecki, J. S., *Theory of Matrix Structural Analysis*. McGraw-Hill, 1968.

[11] Khot, S. M. and Yelve, N. P., Modeling and response analysis of dynamic systems by using ansys and matlab. *Journal of Vibration and Control*, 0(0): 1–6, 2010.

[12] de Marneffe, B. *Active and Passive Vibration Isolation and Damping via Shunted Transducers*. Ph.D. thesis, Université Libre de Bruxelles, 2007.

[13] Fuller, C. R., Elliot, S. J. and Nelson, P. A., *Active Control of Vibration*. Academic Press, Inc., 1997.